Liposome Enhanced Detection of Amyloid Protein Aggregates.

Istvan Kocsis,‡ Elena Sanna‡ and Christopher A. Hunter.*

Department of Chemistry, University of Cambridge, Lensfield Road, Cambridge CB2 1EW (UK). Email: herchelsmith.orgchem@ch.cam.ac.uk.

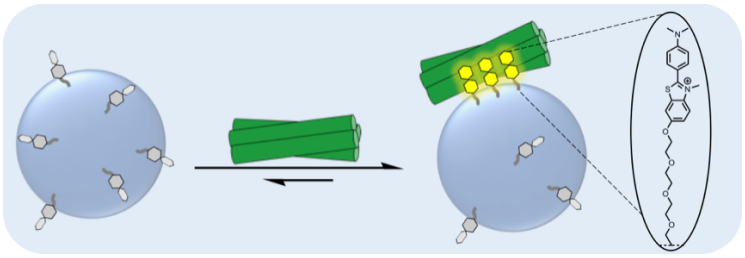

ABSTRACT: Thioflavin-T is used to image amyloid aggregates, because of the excellent turn-on fluorescence properties, but binding affinities are low. By mounting multiple dye units on the surface of a vesicle, the binding affinity for α-synuclein fibrils is increased by three orders of magnitude, and the optical response is increased. Cooperative interactions of the dye head group and lipid with the protein provide a general strategy for the construction of multivalent amyloid probes based on vesicles.

Protein aggregates have been identified in the central nervous systems of patients suffering from degenerative diseases such as Alzheimer's[1], Parkinson's[2] and Huntington's[3], but methods for the early stage detection of these amyloids are limited by the low concentrations present[4] and the low binding affinities of imaging probes.[5] One of the most commonly used dyes for imaging protein aggregates is Thioflavin-T (ThT), which shows an order of magnitude increase in fluorescence intensity on protein binding (Figure 1(a)).[6,7] Multiple binding sites with different binding affinities have been described, but the dissociation constants for the interaction of ThT with protein aggregates are all in the micromolar range.[8,9] Modest increases in binding affinity have been achieved by synthesising multivalent ThT derivatives.[10,11,12] Here we report a supramolecular approach to the assembly of multivalent high contrast probes for protein aggregates. By mounting ThT derivatives on the surface of lipid vesicle membranes, it is possible to obtain a turn-on fluorescent probe for amyloids with nanomolar binding affinity and increased optical brightness compared with ThT (Figure 1(b)).[13,14]

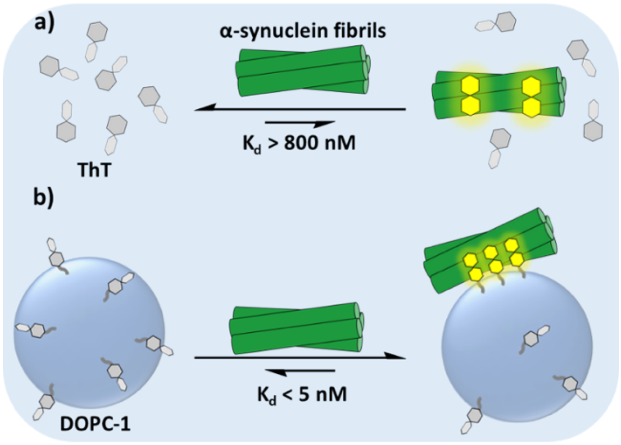

Figure 1. Turn-on fluorescence sensing of amyloid fibrils. a) Low affinity binding (K_d > 800 nM) of standard monomeric ThT. b) High affinity binding (K_d < 5 nM) of multiple ThT head groups anchored in lipid bilayer membranes.

Figure 2 shows the structure of ThT derivative **1** (see ESI for synthetic details). The palmityl chain is a membrane anchor that allows incorporation into vesicles. The ThT headgroup is attached via a short oligoethylene glycol unit to allow the dye to extend into the aqueous solution away from the bilayer interface and access binding sites on protein aggregates.

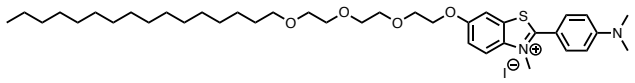

1

Figure 2. Molecular structure of ThT derivative **1**.

Small unilamelar vesicles containing either 1,2-dioleoyl-sn-glycero-3-phosphocholine (DOPC) or a mixture of DOPC and **1** (DOPC•**1**) were prepared by rehydration of lipid films, followed by extrusion through 200 nm diameter pores, and purification by size exclusion chromatography (see ESI for details). The fluorescence spectrum of the DOPC•**1** vesicle solution showed a low intensity emission at 490 nm, comparable to a solution of the parent dye, ThT. However, when the DOPC•**1** vesicles were added to a solution of sonicated α-synuclein fibrils, the fluorescence intensity increased dramatically in a time dependent manner (Figure 3).

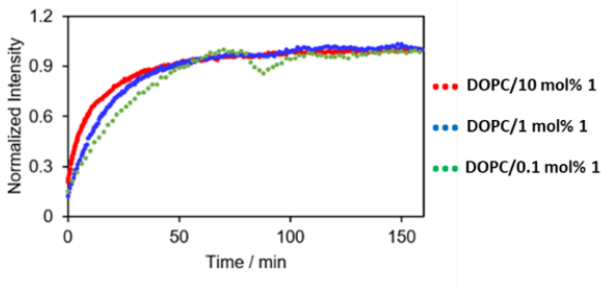

Figure 3. Normalized fluorescence intensity as a function of time after addition of a solution of DOPC vesicles loaded with 10 mol% relative to the lipid (red), 1 mol% (blue) and 0.1 mol% (green) **1** to a 0.1 μM solution of α-synuclein fibrils in PBS 1X (the bulk concentration of **1** was 15 nM in all cases). Excitation at 440 nm and emission at 490 nm.

Equilibrium was established after a period of two hours. The rate of equilibration was independent of the amount of vesicle solution added to the protein, i.e. the bulk concentration of vesicles (see Figure S6). Figure 3 shows that the rate of equilibration increases with the loading of **1**, i.e. the local concentration of **1** in individual vesicles. These observations suggest that the slow process shown in Figure 3 is not equilibration of protein-dye interactions between different vesicles, rather it is equilibration of protein-dye interactions on the surface of individual vesicles.[17]

It is possible that the slow process is due to further aggregation of the α-synuclein fibrils. However, transmission electron microscopy of protein samples exposed to DOPC•**1** vesicles showed no evidence for the formation of larger fibers. Figure 4(c) shows that images of sonicated α-synuclein fibrils incubated with DOPC•**1** vesicles for three hours are very similar to the starting α-synuclein fibrils (Figure 4(a)) and quite different from a sample of fully aggregated α-synuclein fibers (Figure 4(b)).

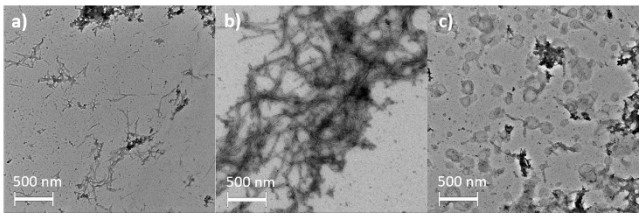

Figure 4. Transmission electron microscopy images of (a) sonicated α-synuclein fibrils, (b) fully aggregated α-synuclein fibres and (c) sonicated α-synuclein fibrils incubated for 3 hours with 150 nM DOPC vesicles loaded with 10 mol % **1** in PBS buffer.

The binding affinity for α-synuclein fibrils was measured by adding increasing amounts of DOPC•**1** vesicles and allowing the solutions to equilibrate for three hours before recording the fluorescence intensity. Figure 5 shows the results of a typical fluorescence titration experiment and the best fit to a 1:1 binding isotherm based on the concentration of **1**. Figure 5(b) compares the fluorescence titration data obtained in the presence and absence of α-synuclein fibrils. The DOPC•**1** vesicles have a low fluorescence emission intensity in the absence of protein, and there is an enhancement of more than an order of magnitude in the fluorescence emission intensity on binding to the fibrils.

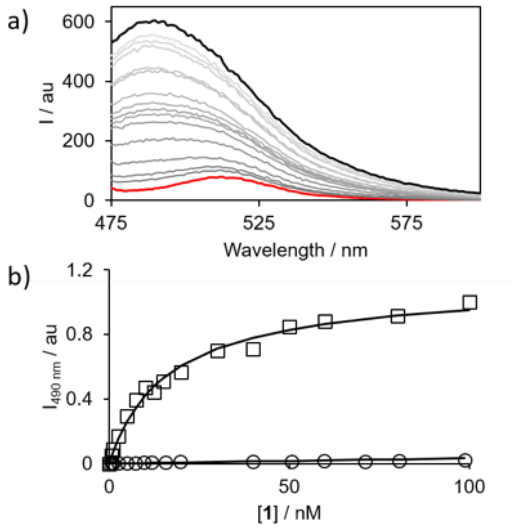

Figure 5. a) Fluorescence spectra for titration of DOPC vesicles containing 10 mol % **1** into 0.1 μM α-synuclein fibrils in PBS 1X (λ_{ex} = 440 nm). The initial spectrum is highlighted in red and the final point of the titration in black. b) Fluorescence emission intensity at λ_{em} = 490 nm for titration of DOPC vesicles containing 10 mol % **1** into 0.1 μM α-synuclein fibrils (squares), and into PBS buffer (circles). The lines are the best fit to a model that accounts for the emission due to the complex between the dye and the protein and for the emission due to the free dye.

Table 1. Dissociation constants (K_d) and fluorescence amplification factors (I_{bound} / I_{free}) for interaction with 0.1 μM α-syn fibrils at pH 7.4 and 298 K measured using fluorescence titrations.[a]

Compound[b]	Lipid	K_d (nM)	I_{bound} / I_{free}
ThT	-	830 ± 80	23 ± 13
1	-	70 ± 20	370 ± 260
1 (10 mol%)	DOPC	15 ± 1	91 ± 43
1 (1 mol%)	DOPC	4 ± 1	10 ± 2

[a] Average values from repeated experiments with standard deviations.
[b] Loading of **1** expressed as molar percentage relative to lipid.

The titration data for addition of the dye to the protein solution and the dilution data for addition of the dye to buffer were simultaneously fit to an isotherm that accounted for the fluorescence emission of the free dye as well as the fluorescence emission of the complex formed when the dye is bound to the α-synuclein fibrils. The dissociation constants for the interaction with α-synuclein fibrils are summarised in Table 1. There is an increase of two orders of magnitude in binding affinity for DOPC•**1** vesicles compared with the parent dye, ThT.[15] Compound **1** also binds α-synuclein fibrils with a reasonably high affinity in the absence of vesicles, which suggests that there are additional binding interactions between hydrophobic regions on the surface of the fibril and the lipid tail. In this case, there was no time-dependent change in the fluorescence intensity, so equilibration of the samples was not required. This observation is consistent with the hypothesis that reorganization of the dyes at the lipid membrane interface is responsible for the slow process shown in Figure 3.

The increase in fluorescence emission intensity associated with binding of the dye to the protein was quantified using the fluorescence amplification factor (I_{bound} / I_{free}). The amplification factor was

calculated as the ratio of the fluorescence emission due to bound and free dye in a solution, which contains free dye at a concentration equal to the dissociation constant for binding to the protein, i.e. when half of the protein binding sites are bound to the dye (see ESI). This parameter provides a useful measure of the relative contrast that can be expected in amyloid imaging experiments using different dyes. The results in Table 1 show that the optical response of **1** is superior to the parent dye, ThT. For DOPC•**1** vesicles, the amplification factor is inversely proportional to the loading of dye in the vesicles. Thus, there is a trade-off between increased binding affinity and reduced amplification factor when the loading of the dye is reduced.

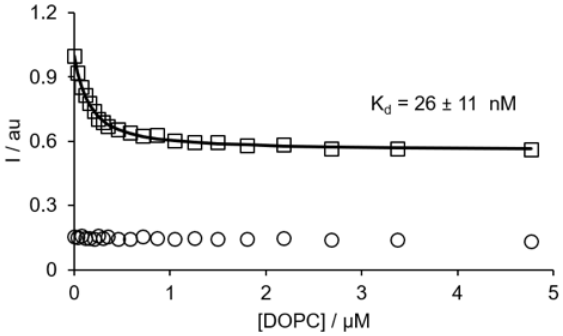

Figure 6. Fluorescence displacement assay for binding of DOPC vesicles to α-synuclein. Fluorescence intensity recorded at 490 nm after addition of DOPC vesicles to solutions containing either 5 μM ThT (circles) or 5 μM ThT with 0.1 μM α-synuclein (squares) in PBS buffer.

Amyloid fibrils are known to interact with lipid bilayers, so the increased binding affinity observed for DOPC•**1** vesicles may be related to cooperative interactions of the protein fibrils with the lipid.[16,17,18,19] For example, the binding affinity reported for theinteraction of α-synuclein fibrils with 1,2-dimyristoyl-sn-glycero-3-phospho-L-serine (DMPS) vesicles is 380 nM.[20] To quantify the interaction of DOPC vesicles with α-synuclein fibrils a ThT displacement assay was used.[20] DOPC vesicles were titrated into a solution of α-synuclein fibrils saturated with ThT. Figure 6 shows that the vesicles displace ThT from the fibrils, leading to an immediate decrease in fluorescence intensity. In this case, the change in fluorescence intensity occurred rapidly on mixing and did not change over time. The data fit well to a 1:1 binding isotherm giving a dissociation constant of 26 ± 11 nM based on the concentration of lipid molecules. However, the DOPC vesicles only displace half of the ThT, and there is significant fluorescence emission from bound ThT at the end of the titration. This result indicates that there are two different ThT binding sites on the α-synuclein fibrils, and the lipids only interact with one of these sites.

The dramatically enhanced affinity for α-synuclein fibrils, which is observed for ThT displayed on the surface of vesicles appears to be the result of cooperative binding interactions between the dye head groups of **1** and the lipid molecules themselves. Figure 7 shows a model that accounts for the observed variations in dissociation constant and fluorescence amplification factor with the loading of **1** in the vesicles. At high loadings, interactions with the dye head groups dominate, leading to a larger optical response, but a lower binding affinity. At low loadings, interactions with the lipid dominate, leading to a higher affinity, but a lower optical response. Binding of α-synuclein fibrils to vesicles is fast, so the time dependence of the optical response observed for DOPC•**1** vesicles is most likely due to slow reorganisation of **1** within the lipid bilayer in order to maximise the cooperative interactions that must be made with both the dye and the lipid. There is evidence that α-synuclein fibrils can insert into lipid bilayers, so it is also possible that the slow reorganization shown in Figure 3 is a result of this process.[22]

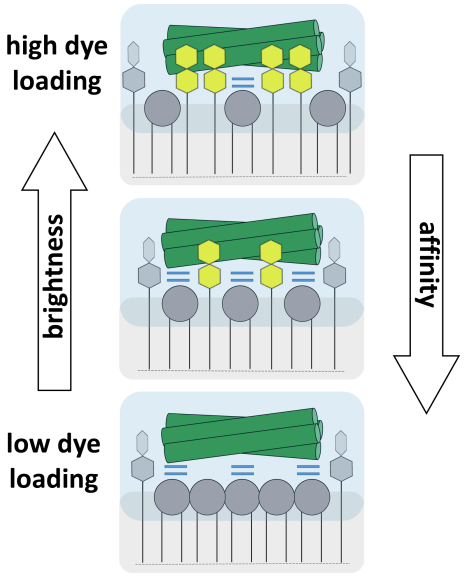

Figure 7. Binding of α-synuclein fibrils to DOPC•**1** vesicles. Competition between binding to the lipid and the dye head groups leads to a trade-off between binding affinity and optical response which depends on the loading of the dye.

In summary, we have shown that mounting a ThT derivative on the surface of vesicles leads to a dramatic enhancement in binding affinity for amyloid aggregates. Cooperative interactions between the dye head groups and the lipids leads to low nanomolar dissociation constants as well as an improved optical response compared with the parent dye, ThT. This supramolecular approach provides a general strategy for the assembly of complex multivalent probes for protein aggregates.

ASSOCIATED CONTENT

Supporting Information

Details of the synthesis and characterisation of **1**, sample preparation, and fluorescence experiments. The Supporting Information is available free of charge on the ACS Publications website.

AUTHOR INFORMATION

Corresponding Author

* Department of Chemistry, University of Cambridge, Lensfield Road, Cambridge CB2 1EW, UK.
E-mail: herchelsmith.orgchem@ch.cam.ac.uk

ACKNOWLEDGMENT

We thank the Engineering and Physical Sciences Research Council (EP/R005397/1 and EP/P008224/1).

REFERENCES

[1] Goedert, M.; Wischik, C. M.; Crowther, R. A.; Walker, J. E.; Klug, A. Cloning and Sequencing of the CDNA Encoding a Core Protein of the Paired Helical Filament of Alzheimer Disease: Identification as the Microtubule-Associated Protein Tau. *Proc. Natl. Acad. Sci.* **1988**, *85* (11), 4051–4055. https://doi.org/10.1073/pnas.85.11.4051.

[2] Kalia, L. V.; Kalia, S. K.; McLean, P. J.; Lozano, A. M.; Lang, A. E. α-Synuclein Oligomers and Clinical Implications for Parkinson Disease.

Ann. Neurol. **2013**, *73* (2), 155–169. https://doi.org/10.1002/ana.23746.

[3] Poirier, M. A.; Jiang, H.; Ross, C. A. A Structure-Based Analysis of Huntingtin Mutant Polyglutamine Aggregation and Toxicity: Evidence for a Compact Beta-Sheet Structure. *Hum. Mol. Genet.* **2005**, *14* (6), 765–774. https://doi.org/10.1093/hmg/ddi071.

[4] Lue, L.-F.; Kuo, Y.-M.; Roher, A. E.; Brachova, L.; Shen, Y.; Sue, L.; Beach, T.; Kurth, J. H.; Rydel, R. E.; Rogers, J. Soluble Amyloid β Peptide Concentration as a Predictor of Synaptic Change in Alzheimer's Disease. *Am. J. Pathol.* **1999**, *155* (3), 853–862. https://doi.org/10.1016/S0002-9440(10)65184-X.

[5] Strømland, Ø.; Jakubec, M.; Furse, S.; Halskau, Ø. Detection of Misfolded Protein Aggregates from a Clinical Perspective. *J. Clin. Transl. Res.* **2016**, *2* (1), 11–26.

[6] Biancalana, M.; Koide, S. Molecular Mechanism of Thioflavin-T Binding to Amyloid Fibrils. *Biochim. Biophys. Acta* **2010**, *1804* (7), 1405–1412. https://doi.org/10.1016/j.bbapap.2010.04.001.

[7] Jung, S. J.; Park, Y. D.; Park, J. H.; Yang, S. D.; Hur, M. G.; Yu, K. H. Synthesis and Evaluation of Thioflavin-T Analogs as Potential Imaging Agents for Amyloid Plaques. *Med. Chem. Res.* **2013**, *22* (9), 4263–4268. https://doi.org/10.1007/s00044-012-0414-2.

[8] Sidhu, A.; Vaneyck, J.; Blum, C.; Segers-Nolten, I.; Subramaniam, V. Polymorph-specific distribution of binding sites determines thioflavin-T fluorescence intensity in α-synuclein fibrils. *Amyloid*, **2018**, *25* (3), 189-196. https://doi.org/10.1080/13506129.2018.1517736.

[9] Groenning, M. Binding mode of Thioflavin T and other molecular probes in the context of amyloid fibrils—current status. *J. Chem. Biol.* **2010**, *3*, 1-18. https://doi.org/10.1007/s12154-009-0027-5.

[10] Qin, L.; Vastl, J.; Gao, J. Highly Sensitive Amyloid Detection Enabled by Thioflavin T Dimers. *Mol. Biosyst.* **2010**, *6* (10), 1791–1795. https://doi.org/10.1039/C005255H.

[11] Capule, C. C.; Brown, C.; Olsen, J. S.; Dewhurst, S.; Yang, J. Oligovalent Amyloid-Binding Agents Reduce SEVI-Mediated Enhancement of HIV-1 Infection. *J. Am. Chem. Soc.* **2012**, *134* (2), 905–908. https://doi.org/10.1021/ja210931b.

[12] Hunter, C. A.; Anderson, H. L. What Is Cooperativity? *Angew. Chem. Int. Ed.* **2009**, *48* (41), 7488–7499. https://doi.org/10.1002/anie.200902490.

[13] Lopez-Fontal, E.; Grochmal, A.; Foran, T.; Milanesi, L.; Tomas, S. Ship in a Bottle: Confinement-Promoted Self-Assembly. *Chem. Sci.* **2018**, *9* (7), 1760–1768. https://doi.org/10.1039/C7SC04553K.

[14] Ding, Y.; Williams, N. H.; Hunter, C. A. A Synthetic Vesicle-to-Vesicle Communication System. *J. Am. Chem. Soc.* **2019**, *141* (44), 17847–17853. https://doi.org/10.1021/jacs.9b09102.

[15] Xu, M.; Ren, W.; Tang, X.; Hu, Y.; Zhang, H. Advances in Development of Fluorescent Probes for Detecting Amyloid-β Aggregates. *Acta Pharmacol. Sin.* **2016**, *37* (6), 719–730. https://doi.org/10.1038/aps.2015.155.

[16] Dubois, V.; Serrano, D.; Seeger, S. Amyloid-β Peptide–Lipid Bilayer Interaction Investigated by Supercritical Angle Fluorescence. *ACS Chem. Neurosci.* **2019**, *10* (12), 4776–4786. https://doi.org/10.1021/acschemneuro.9b00264.

[17] Chang, C.-C.; Edwald, E.; Veatch, S.; Steel, D. G.; Gafni, A. Interactions of Amyloid-β Peptides on Lipid Bilayer Studied by Single Molecule Imaging and Tracking. *Biochim. Biophys. Acta* **2018**, *1860* (9), 1616–1624. https://doi.org/10.1016/j.bbamem.2018.03.017.

[18] Pineda, A.; Burré, J. Modulating membrane binding of α-synuclein as a therapeutic strategy. *Proc. Natl. Acad. Sci.*, **2017**, *114* (6), 1223-1225. http://doi.org/10.1073/pnas.1620159114.

[19] Dikiy, I.; Eliezer, D. Folding and misfolding of alpha-synuclein on membranes. *Biochim. Biophys. Acta*, **2012**, *1818*, 1013-1018. http://doi.org/10.1016/j.bbamem.2011.09.008.

[20] Galvagnion, C.; Buell, A. K.; Meisl, G.; Michaels, T. C. T.; Vendruscolo, M.; Knowles, T. P. J.; Dobson, C. M. Lipid Vesicles Trigger α-Synuclein Aggregation by Stimulating Primary Nucleation. *Nat. Chem. Biol.* **2015**, *11* (3), 229–234. https://doi.org/10.1038/nchembio.1750.

[21] Jamroskovic, J.; Livendahl, M.; Eriksson, J.; Chorell, E.; Sabouri, N. Identification of Compounds That Selectively Stabilize Specific G-Quadruplex Structures by Using a Thioflavin T-Displacement Assay as a Tool. *Chem. – Eur. J.* **2016**, *22* (52), 18932–18943. https://doi.org/10.1002/chem.201603463.

[22] Tosatto, L.; Andrighetti, A. O.; Plotegher, N.; VAntonini, V.; Tessari, I.; Ricci, L; Bubacco, L.; Dalla Serra, M. Alpha-synuclein pore forming activity upon membrane association. *Biochim. Biophys. Acta*, **2012**, *1818*, 2876-2883. https://doi.org/10.1016/j.bbamem.2012.07.007.